



Evolution of physical properties of amorphous Fe–Ni–Nb–B alloys with different Ni/Fe ratio upon thermal treatment

G. Vlasak^{a,*}, P. Svec^a, M. Kuzminski^b, A. Slawska-Waniewska^b, B. Butvinova^a, P. Butvin^a, J. Hosko^a

^a Institute of Physics, Slovak Academy of Sciences, Dubravská Cesta 9, 845 11 Bratislava, Slovakia

^b Institute of Physics, Polish Academy of Sciences, 02 668 Warsaw, Poland

ARTICLE INFO

Article history:

Received 2 July 2010

Received in revised form

10 December 2010

Accepted 15 December 2010

Available online 22 December 2010

Keywords:

Amorphous materials

Magnetostriction

Magneto-optic Kerr effect

Soft magnetic materials

ABSTRACT

Amorphous ribbons (Fe–Ni)₈₁Nb₇B₁₂ with Ni/Fe = 0, 1/6, 1/3 and 1 were prepared by planar flow casting. Thermal treatment of samples was performed in vacuum at temperatures chosen to map the evolution of selected properties in the course of transformation from amorphous state. The coefficient of thermal dilatation exhibits changes at temperatures close to the glass transition, Curie and crystallization temperatures; these effects are enhanced or suppressed by cyclic thermal treatments up to the vicinity of these temperatures. The values of saturation magnetostriction λ_s allow to infer about processes taking place in the investigated materials, especially with respect to formation of new magnetic phases or magnetic anisotropy.

Complex processes of structural transformations induced by thermal treatment are strongly affected by Ni percentage. A transitional, magnetically harder phase, which is formed at lower temperatures preferentially near surfaces of the Ni-richest alloy, produces characteristic hysteresis loop shape. This shape disappears after annealing at higher temperatures and enables the material to show the lowest coercivity of the whole alloy series. The saturation magnetic polarization reflects mainly the resulting Curie temperature, which falls with increasing Ni percentage. Magnetic hysteresis loops were also used in the study of dynamics of magnetic domains by MOKE. Domain shape evolution is shown in dependence on composition and thermal treatment as well as a function of applied magnetic field, ranging from remanent sample state to magnetic saturation.

© 2010 Elsevier B.V. All rights reserved.

1. Introduction

Alloys based on iron and nickel constitute primary metallic materials and are in the constant focus of interest in physical and materials research as well as in industrial applications, representing the class of construction materials as well as of advanced materials with unique properties. Alloying of Fe and Ni together with further additions of specific elements leads to systems which are attractive from mechanical, magnetic and structural point of view. Several combinations of alloys based on Fe and Ni are soft magnetic materials.

Rapidly quenched system based on Fe–Ni–P–B with respect to the transition from ferromagnetic to paramagnetic state has been studied previously [1]. Our present work is oriented on the Fe–Ni–Nb–B system with constant amounts of B and Nb and varying ratio of Ni to Fe. Changes of the Curie temperature, magnetic hysteresis loops, magnetostriction and magnetic domains dynamics are investigated on samples after specific thermal treatment.

2. Experimental

Samples with the composition (Fe–Ni)₈₁Nb₇B₁₂ having the ratio Ni/Fe = 0, 1/6, 1/3 and 1/1 were prepared by planar flow casting in form of ribbons ~20 μ m thick with 6 mm width. The as-quenched samples were in amorphous state as confirmed by X-ray diffraction and transmission electron microscopy. Ribbon samples were used for dilatation measurements under special heating regimes. The thermal regime has been as follows: as-quenched samples were linearly heated with the heating rate of 5 K/min to 500 °C where they were isothermally annealed for 30 min (curves labelled as 1 in Fig. 1a–d). After controlled cooling with the same rate the samples were again linearly heated to 550 °C followed by another 30 min annealing (curves labelled as 2 in Fig. 1a–d) and controlled cooling. The third linear heating cycles with the same heating rate up to 550 °C are labelled as 3. The values of T_C were determined as local extremes of the temperature coefficients of dilatation; the values of T_g were determined in a similar manner.

Magnetostriction, alongside with magnetization, is another important property of magnetic materials. It is generally accepted that amorphous metallic alloys represent isotropic medium where the following relations for parallel λ_{par} , perpendicular λ_{perp} and saturation magnetostriction λ_s , hold as $\lambda_s = 2/3 (\lambda_{par} - \lambda_{perp})$. The values of λ_{par} and λ_{perp} are determined from the field dependencies of magnetostrictions $\lambda(H)$ in parallel and perpendicular directions to the applied magnetic field H [2–4]. Upon thermal treatment of amorphous metallic alloys either relaxation processes or transformations from amorphous into crystalline state take place (at higher temperatures) and the assumption about the isotropic medium is no longer fully valid; the values of λ_{par} and λ_{perp} are affected by the changes of the structure.

The alloys selected for the present study contain magnetic atoms of Fe and Ni as major constituent elements, thus the investigation of these materials included

* Corresponding author.

E-mail addresses: Gabriel.Vlasak@savba.sk, fyzivlas@savba.sk (G. Vlasak).

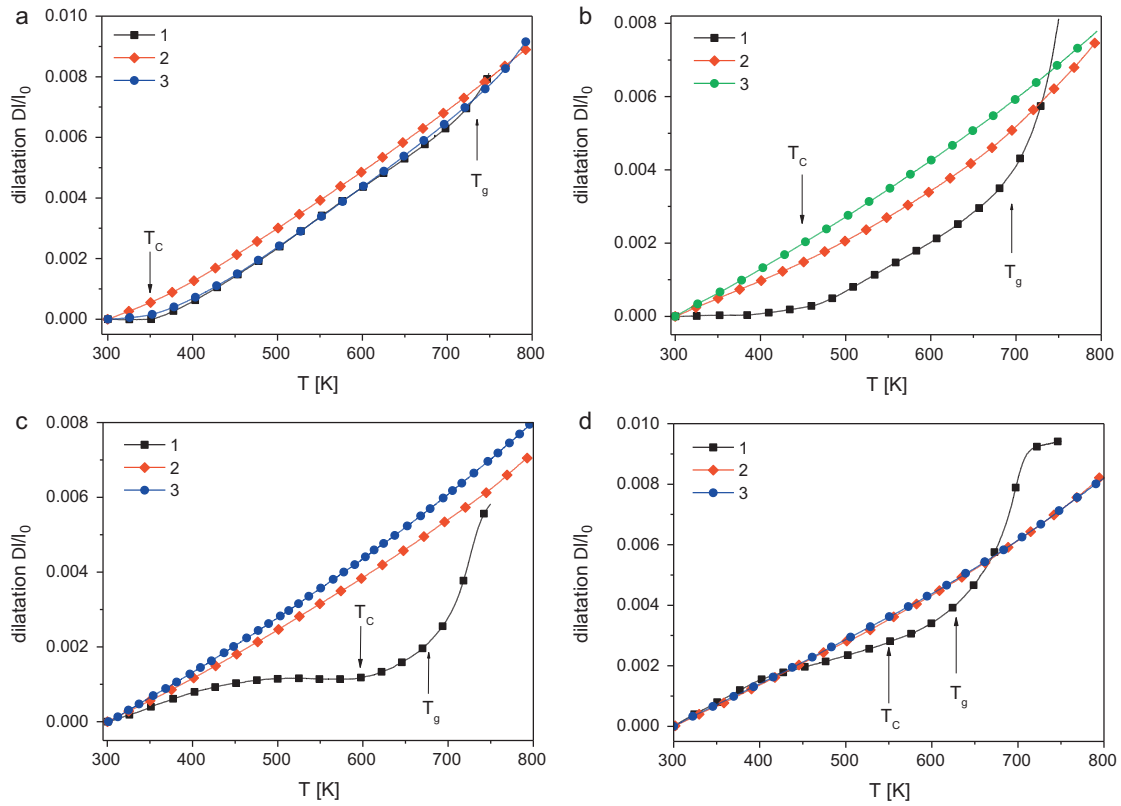


Fig. 1. Dilatation of Fe–Ni–Nb–B alloys in as-quenched state (curve 1) and after subsequent thermal treatment at 500 °C/0.5 h and cooling (curve 2) and after subsequent thermal treatment at 550 °C/0.5 h and cooling (curve 3). (a) $\text{Fe}_{81}\text{Nb}_7\text{B}_{12}$, (b) $(\text{Fe}_6\text{Ni}_1)_{81}\text{Nb}_7\text{B}_{12}$, (c) $(\text{Fe}_3\text{Ni}_1)_{81}\text{Nb}_7\text{B}_{12}$, (d) $(\text{Fe}_1\text{Ni}_1)_{81}\text{Nb}_7\text{B}_{12}$. Heating and cooling rates 5 K/min. The positions of Curie temperatures T_C and glass transition temperatures T_g are indicated by arrows.

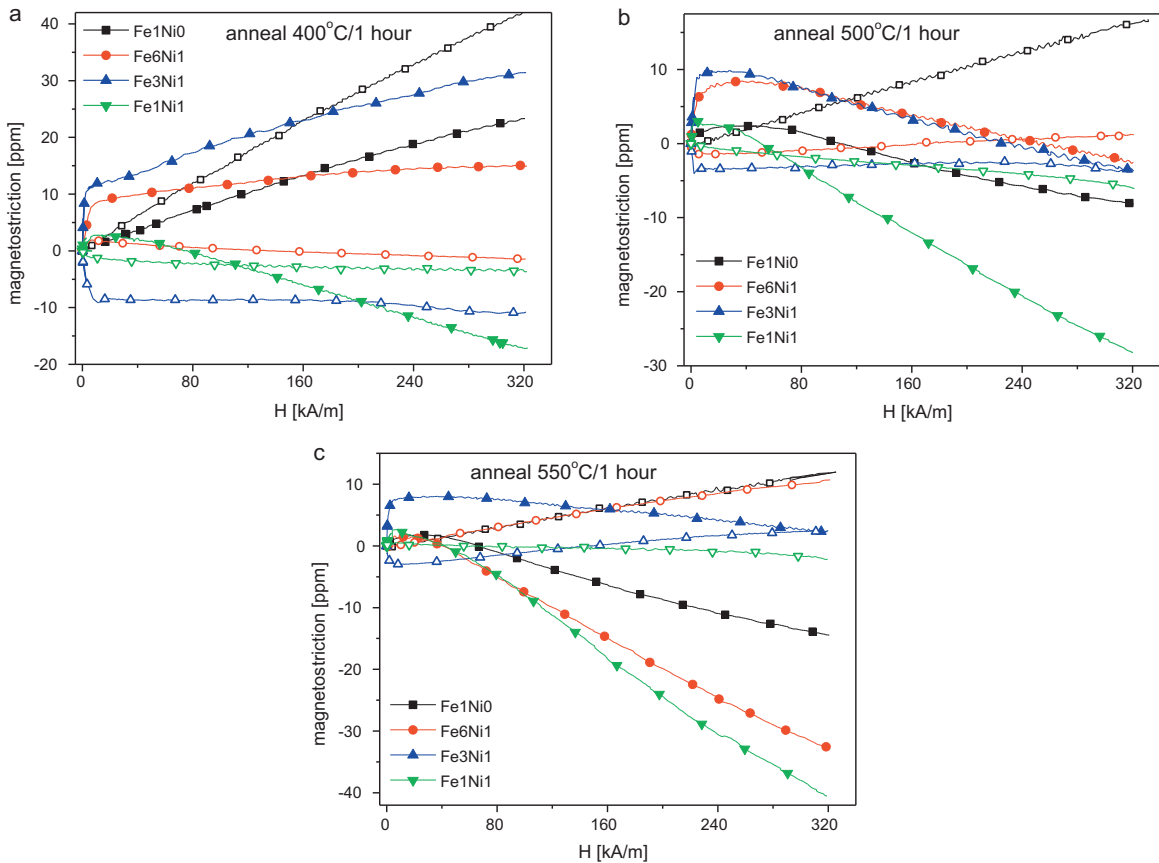


Fig. 2. Field dependencies of magnetostrictions in parallel and perpendicular directions for $(\text{Fe})_{81}\text{Nb}_7\text{B}_{12}$, $(\text{Fe}_1\text{Ni}_1)_{81}\text{Nb}_7\text{B}_{12}$, $(\text{Fe}_3\text{Ni}_1)_{81}\text{Nb}_7\text{B}_{12}$ and $(\text{Fe}_6\text{Ni}_1)_{81}\text{Nb}_7\text{B}_{12}$ upon thermal treatment at (a) 400 °C, (b) 500 °C and (c) 550 °C for 1 h in vacuum. Full symbols – $-\lambda_{\text{par}}$, open symbols – $-\lambda_{\text{perp}}$.

also their magnetic behaviour and properties. Among these are magnetization processes studied by means of computer-aided magneto-optic Kerr effect (MOKE) and by magnetization measurements, specifically hysteresis loops.

Strips of 9 cm length were used for magnetic measurements. Hysteresis loops were recorded using a digitizing hysteresisgraph at standard ac (21 Hz) sinusoidal H excitation in Helmholtz drive coils. The excitation and measurement direction is aligned parallel to the ribbon long axis to use the lowest demagnetization factor D of the strip. The internal field H_i is computed according to the standard relation $H_i = H_e - DJ/\mu_0$. The pick-up coils are arranged so that the induced voltage is proportional to magnetic polarization J and not to induction B .

The static domain structure of the investigated metallic glass ribbons was studied by means of computer-aided magneto-optic Kerr effect (MOKE). The method maps the domain structure on the surface of the samples and the signal-to-noise ratio is increased by averaging and subtracting a suitable background from the recorded image [5–7].

Two polarization orientations along the long axis of the ribbons were used to obtain information on the magnetization components – in remanent state after magnetization in one direction, denoted as (+) remanence, and after magnetization in opposite direction, denoted as (–) remanence. All principal directions (long ribbon axis, maximum magneto-optical sensitivity, bias field) are vertical with respect to the images. The full ribbon width (6 mm) is visible in the horizontal direction of the images.

3. Results and discussion

Temperature dependencies of dilatation measurements (Fig. 1a–d) point to the physical processes, which take place upon thermal treatment. One of the important observations is the shift of the Curie temperature T_C . The positions of the Curie temperature T_C and glass transition temperature T_g of as-quenched samples can be determined from the changes of the slope of curves 1. These temperatures are for all samples below 500 °C. These temperatures, however, cannot be seen on curves 2 and 3 due to the transformation processes which have already taken place at 500 or 550 °C. From the mechanical point of view, changes of thermal coefficient of dilatation are observed as well. Both effects

Table 1

The values of saturation magnetostriction and coercivity for the different sample compositions after thermal treatment for 1 h at the indicated temperatures.

Alloy Ni/Fe	λ_s [ppm]			H_c (21 Hz) [A/m]		
	400 °C	500 °C	550 °C	400 °C	500 °C	550 °C
0	0	5	3.3	4.0	700	137
1/6	4.5	8.83	3.36	5.5	4.7	9.3
1/3	12.5	10.2	8.33	5.1	6.2	11.4
1/1	4.66	4.83	6.67	14.4	3.3	4.7

are due to the formation of the crystalline phases above 500 °C. For compositions with Ni/Fe = 0, 1/6 and 1/3 the crystalline phase formed during the applied thermal treatment is nanocrystalline bcc-Fe embedded in amorphous remains. For Ni/Fe = 1/1 the formation of fcc-Fe(Ni) and (Fe–Ni)₂₃B₆ phases with small traces of bcc-Fe(Ni) was observed [8,9].

The dependencies of $\lambda_{\text{par}}(H)$ and $\lambda_{\text{perp}}(H)$ for different thermal treatments are shown in Fig. 2a–c. Magnetostriction measurements of as-quenched samples measured at room temperature indicate that the alloy with Ni/Fe = 0 is close to paramagnetic state ($T_C \sim 80$ °C) – the value of room-temperature λ_s is nearly zero [8]. All compositions are ferromagnetic in amorphous state. After thermal treatment at 500 and 550 °C formation of crystalline phases further affect the shapes of the dependencies of $\lambda_{\text{par}}(H)$ and $\lambda_{\text{perp}}(H)$.

The values of saturation magnetostriction and coercivity for the samples after thermal treatment are shown in Table 1. Substitution of Fe by Ni seems to improve soft magnetic properties, especially the coercivity, of the Fe–Ni–Nb–B alloys after thermal treatment at 500 °C. A slight increase of saturation magnetostriction values, which, however, are rather small, with increased Ni content up to Ni/Fe \sim 1/3 does not seem to affect these quantities too much, pos-

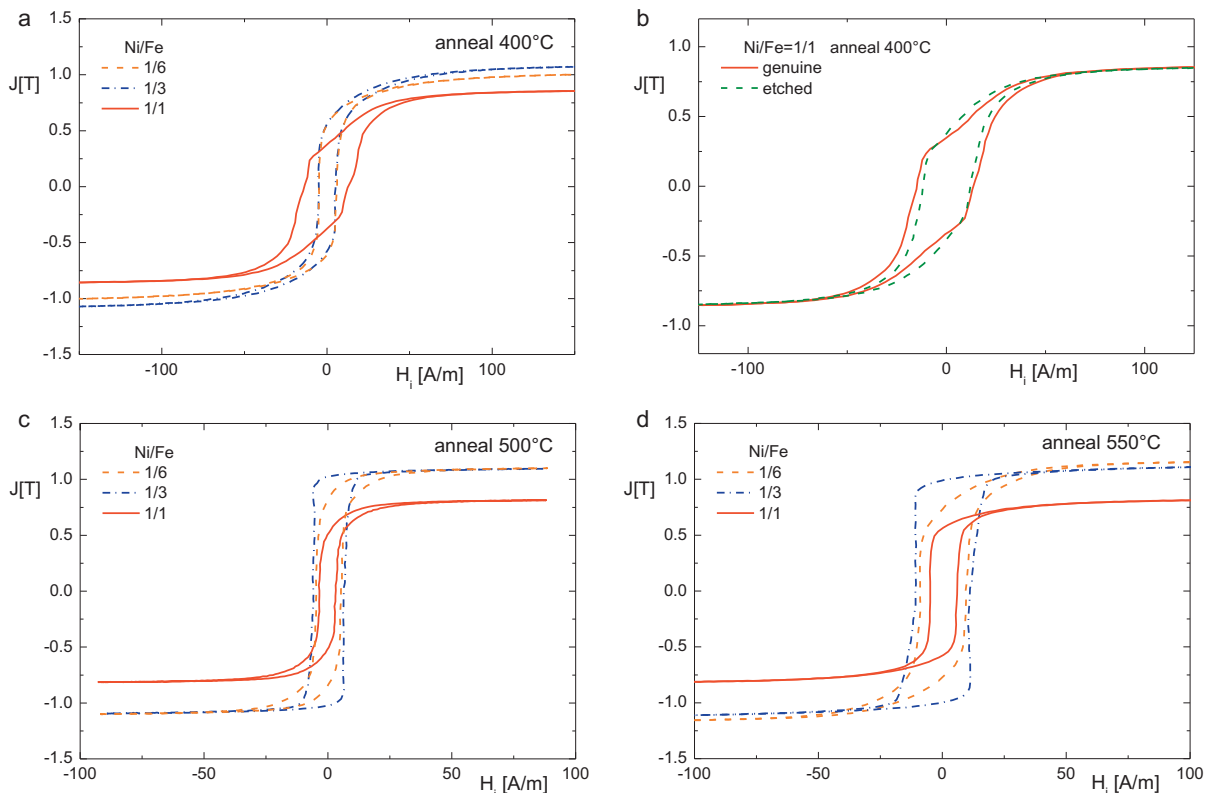


Fig. 3. (a) Hysteresis loops of Fe–Ni–Nb–B alloys annealed at 400 °C 1 h in vacuum; (b) comparison of loops of 400 °C 1 h vacuum annealed Ni/Fe = 1/1 before (= genuine) and after etching; (c) hysteresis loops of Fe–Ni–Nb–B alloys annealed at 500 °C 1 h in vacuum; (d) hysteresis loops of Fe–Ni–Nb–B alloys after 550 °C 1 h vacuum annealing.

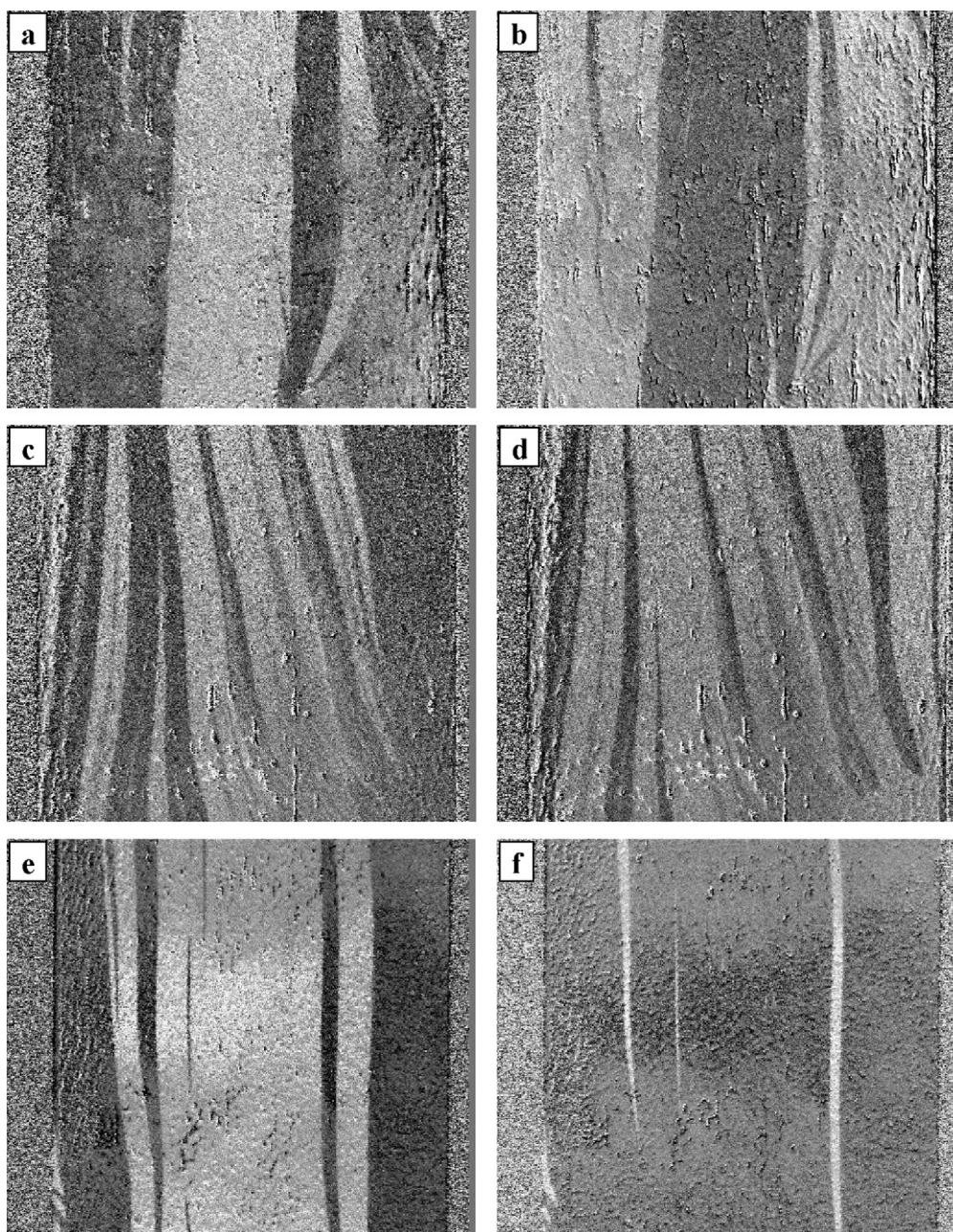


Fig. 4. MOKE domain structure of Fe–Ni–Nb–B samples in remanent states annealed at 500 °C for 1 h: $(\text{Fe}_6\text{Ni}_1)_{81}\text{Nb}_7\text{B}_{12}$ (–) remanence (a), (+) remanence (b); $(\text{Fe}_3\text{Ni}_1)_{81}\text{Nb}_7\text{B}_{12}$ (c) in remanent state with (–) remanence and (d) bias + 40 A/m; $(\text{Fe}_1\text{Ni}_1)_{81}\text{Nb}_7\text{B}_{12}$ (e) in remanent state with (–) remanence and (f) bias + 40 A/m. Please, consult experimental for orientation of sample, field and MOKE sensitivity.

sibly also due to the change of the microstructure and chemical composition of the nanograins present in the amorphous matrix and possibly also due to decreasing size of the nanograins [9]. The Ni-free basic alloy has already been studied in detail [10] and its properties are not targeted in this work. Nevertheless it could be recalled that the significant variation of the coercivity with the annealing temperature (Table 1) was ascribed to the vicinity of the resulting amorphous-residual Curie temperature to measurement temperature, which results in “strong decoupling” [10] of nanocrystalline grains at these conditions.

Hysteresis loops of the investigated alloys measured after isothermal annealing at selected temperatures (400, 500 and 550 °C) are shown in Fig. 3a–d. The magnetic hysteresis loops

essentially lost their as-cast character (poor saturation) [8] demonstrating substantial relaxation of the as-cast internal stresses during the 1 h 400 °C vacuum annealing – Fig. 3a. Apart from Ni/Fe = 1/1, the saturation magnetic polarization keeps the order of alloys the same as observed for Curie temperature T_C of the as-cast state [9] – higher J_s goes with higher T_C . Ni/Fe = 1/1 shows the highest amorphous T_C (~300 °C), but this alloy displays the lowest J_s that coincides with the peculiar loop shape. Since this material, if crystallized, does not exhibit any crystalline phase with T_C exceeding ~450 °C [9], it appears as if some phase with lower T_C or even paramagnetic phase started to precipitate during the 400 °C anneal. Since the paramagnetic NiFe boride is only reported [11] after a 600 °C annealing, there is no such new phase identified

after the 400 °C annealing [11]. If annealed in a gaseous ambience, all the alloys of the studied system show preferred surface crystallization and similar tilted loops. To test the suspect surface-stress effect that engages magnetoelastic interaction, surfaces of the vacuum-annealed Ni/Fe = 1/1 were removed by etching in an acidic lye. After removing ~2% from the genuine 18 μm thickness, the peculiar edged character of the loop was visibly reduced – Fig. 3b. Moreover, the tilt was slightly reduced too. This is what could be expected, if a part of surface layer, which compresses – squeezes the ribbon interior of a positively magnetostrictive Si-poor or Si-free material is removed [12]. After 500 °C annealing, the loops in Fig. 3c already show good saturation and low dynamic (21 Hz) coercivity – just Ni/Fe = 1/1 bearing the well identified fcc-FeNi phase [11] is the best with 3.3 A/m. Further slight lowering of J_s and vanishing of the surface-stress effect is observed for this alloy, whereas the other two alloys meet with their rising saturation in accord with the thermomagnetic record [9]. The accordance applies also to the 550 °C annealing (Fig. 3d), where the saturation of Ni/Fe = 1/6 already surpasses that of Ni/Fe = 1/3 due to more extensive precipitation of the crystalline phase [11] with higher T_C . However the coercivity generally rises. Since no competing effects, as the abovementioned surface-stress one reveal their participation, the minute loss of magnetic softness is to be looked for solely in the complex consequences of progressing crystallization, although without a noteworthy grain growth or clear correlation to the observed interfacial phase that surrounds the grains [11]. The different shape of Ni/Fe = 1/3 loops coincides with the observed domain structure (see Fig. 4c and d), which shows significantly thinner domains diverging from the ribbon axis. This points to stronger anisotropy with a transversal component where the higher magnetostriction of this alloy could be the reason.

MOKE images of the surface domain structure observed on the shiny side of the investigated ribbons are shown in Fig. 4a–f. The images of magnetic domains indicate that their formation is preferentially in form of strips oriented along the long axis of the ribbon samples; their motion in external magnetic field is in the direction perpendicular to the long ribbon axis, as observed during the changes of the polarity of the external magnetic field applied prior to observations. The domain structure is typical of low-anisotropy materials with the easy direction aligned preferentially along the long ribbon axis. No closure domains were detected although slight branching and deviation of 180° walls from the longitudinal direc-

tion point to a minor off-axis anisotropy component in Ni/Fe = 1/3 (Fig. 4c and d).

4. Conclusions

Apart from the annealing at 400 °C where possibly a transitional phase starts to form preferentially at ribbon surfaces, the Ni/Fe = 1/1 exhibits slightly diminishing saturation and lowest coercivity at higher annealing temperatures. All the other alloys show the saturation rising with the annealing temperature that corresponds to advancing precipitation of crystalline phases with higher Curie temperature. Vacuum annealing enables the low easy-ribbon-axis anisotropy to dominate and give the best soft-magnetic properties after 500 °C annealing.

The complex research of Fe–Ni-based amorphous metallic alloys gives possibility of their use in the material development and application.

Acknowledgments

Support of the Agency of the Ministry of Education of the Slovak Republic for the Structural Funds of the EU (CEKOMAT I, ITMS 26240120006) is gratefully acknowledged. This work was supported by the projects VEGA 2/0157/08, 2/0156/08, 2/7193, 2/0111/11, APVV-0413-06, COST-031-06 (P17), SK-CN-0021-07 and also by the CEX “Nanosmart”.

References

- [1] H.H. Liebermann, C.D. Graham, P.J. Flanders, IEEE Trans. Magn. MAG-13 (1977) 1541.
- [2] E. Tremolet de Lacheisserie, J. Magn. Magn. Mater. 31–36 (1983) 1491.
- [3] G. Vlasak, J. Magn. Magn. Mater. 215–216 (2000) 479–481.
- [4] G. Vlasak, P. Švec, J. Electr. Eng. 55 (2004) 81.
- [5] A. Honda, K. Shirai, IEEE Trans. Magn. 17 (1981) 3096.
- [6] M. Kuzminski, J. Fink-Finowicki, A. Siemko, Electron. Horizon 53 (1992) 87.
- [7] M. Kuzminski, J. Fink-Finowicki, A. Siemko, Acta Magn. (Suppl. 90) (1990) 147.
- [8] G. Vlasák, P. Švec, M. Kuzminski, A. Slawska-Waniewska, B. Butvinová, P. Butvin, J. Magn. Magn. Mater. 322 (2010) 2047.
- [9] J. Turčanová, J. Marcin, J. Kováč, D. Janičkovič, P. Švec, I. Škorvánek, J. Phys.: Conf. Ser. 144 (2009) 012065.
- [10] I. Škorvánek, P. Švec, J.-M. Grenèche, J. Kováč, J. Marcin, R. Gerling, J. Phys. Condens. Matter 14 (2002) 4717–4736.
- [11] P. Švec, M. Miglierini, J. Dekan, J. Turčanová, G. Vlasák, I. Škorvánek, D. Janičkovič, P. Švec Sr., IEEE Trans. Magn. 46 (2010) 412.
- [12] P. Butvin, B. Butvinová, J.M. Silveyra, M. Chromčková, D. Janičkovič, J. Sitek, P. Švec, G. Vlasák, J. Magn. Magn. Mater. 322 (2010) 3035.